J. Fluid Mech. (1998), *vol.* 364, *pp.* 163–185. Printed in the United Kingdom

Kinetic theory for a vibro-fluidized bed

By V. KUMARAN

Department of Chemical Engineering, Indian Institute of Science, Bangalore 560 012, India

(Received 25 January 1997 and in revised form 5 January 1998)

The velocity distribution function for a two-dimensional vibro-fluidized bed of particles of radius r is calculated using asymptotic analysis in the limit where (i) the dissipation of energy during a collision due to inelasticity or between successive collisions due to viscous drag is small compared to the energy of a particle and (ii) the length scale for the variation of density is large compared to the particle size. In this limit, it is shown that the parameters $\epsilon_G = rg/T_0$ and $\epsilon = U_0^2/T_0 \ll 1$, and ϵ and ϵ_G are used as small parameters in the expansion. Here, g is the acceleration due to gravity, U_0 is the amplitude of the velocity of the vibrating surface and T_0 is the leading-order temperature (divided by the particle mass). In the leading approximation, the dissipation of energy and the separation of the centres of particles undergoing a binary collision are neglected, and the system is identical to a gas of rigid point particles in a gravitational field. The leading-order particle number density is given by the Boltzmann distribution $\rho_0 \propto \exp(-gz/T_0)$, and the velocity distribution function is given by the Maxwell–Boltzmann distribution $f(\boldsymbol{u}) = (2\pi T_0)^{-1} \exp[-\boldsymbol{u}^2/(2T_0)]$, where $\boldsymbol{u}$ is the particle velocity. The temperature cannot be determined from the leading approximation, however, and is calculated by a balance between the rate of input of energy at the vibrating surface due to particle collisions with this surface, and the rate of dissipation of energy due to viscous drag or inelastic collisions. The first correction to the distribution function due to dissipative effects is calculated using the moment expansion method, and all non-trivial first, second and third moments of the velocity distribution are included in the expansion. The correction to the density, temperature and moments of the velocity distribution are obtained analytically. The results show several systematic trends that are in qualitative agreement with previous experimental results. The correction to the density is negative at the bottom of the bed, increases and becomes positive at intermediate heights and decreases exponentially to zero as the height is increased. The correction to the temperature is positive at the bottom of the bed, and decreases and assumes a constant negative value as the height is increased. The mean-square velocity in the vertical direction is greater than that in the horizontal direction, thereby facilitating the transport of energy up the bed. The difference in the mean-square velocities decreases monotonically with height for a system where the dissipation is due to inelastic collisions, but it first decreases and then increases for a system where the dissipation is due to viscous drag.

1. Introduction

The properties of vibrated and fluidized granular materials have been of interest in technological applications in solids transportation, handling and processing. Many of these processes involve the vibration of a granular material from below. In dense vibrated beds at low base velocity the particles form a layered structure and remain in

contact for extended periods of time. However, as the number of layers of particles is decreased and the velocity of the vibrating surface is increased, the energy transmitted to the material from the vibrating surface results in a vigorous motion of the particles, where the time of contact between the particles during a binary collision is small compared to the time between successive collisions. In this regime, momentum and energy are transmitted due to instantaneous collisions between the particles, and the sustained frictional contact is not present. These materials exhibit unusual properties, such as liquid-like streaming motion and wave propagation (Savage 1988; Goldshtein *et al.* 1995), and gas-like density variations and shock waves (Warr, Huntley & Jacques 1995; Goldshtein *et al.* 1995) for certain parameter regimes. The development of statistical descriptions for these types of behaviour involves averaging over the 'microscopic' laws for the particle motion to obtain 'macroscopic' conservation equations for the flow. A statistical description for the uniformly fluidized state of a vibrated bed, using methods from the kinetic theory of gases, is the subject of the present analysis.

There has been a lot of research on the properties and the stability of gas-fluidized beds, where a gas is passed upward through a bed of particles, and the vigorous motion of the particles is caused by the drag force exerted by the gas. The stability of the uniformly fluidized state of the bed has been of interest for some time, and the earliest work in this area was carried out by Jackson (1963) who showed, using a simple continuum description, that the uniformly fluidized state of the bed is always unstable to density fluctuations. Since then, there has been a lot of work on continuum descriptions and stability analyses of the uniform state of a fluidized bed (see, for example, Didwania & Homsy 1982; Batchelor 1988; and the review by Jackson 1985). However, there is still no consensus on the appropriate continuum description of a fluidized bed, and its stability. There have been fewer attempts to obtain a statistical description, by averaging over the microscopic dynamics of the particles, possibly due to the complex interactions between the turbulent gas flow and the particle motion. The description of particle dynamics in a vibrated fluidized bed is simpler, because the fluidization takes place due to the vibration of the bottom surface.

There have been many experimental and theoretical studies of the motion of vibrated granular materials, but there have been fewer attempts at obtaining a microscopic description for the motion of the material. Savage (1988) conducted experiments on a vibrated bed of polystyrene spheres. The bed was vibrated at the bottom, with a maximum amplitude at the centre of the bed and zero amplitude at the sides, and a circulatory streaming pattern was observed. The author used a model for a granular material similar to that of Jenkins & Savage (1983) for the flow of smooth, inelastic spherical particles undergoing collisions, and the circulation was treated in a manner similar to the acoustic motion in gases. More recently, Goldshtein *et al.* (1995) have considered the dynamics of a granular material vibrated uniformly from below. They have observed three types of behaviour: a solid-like state where the entire granular material behaves as a plastic body; a liquid-like regime where there are transverse waves on the surface of the material; and a gas-like state where there are expansion–compression waves propagating upward. The authors propose a description for the gas-like state using equations similar to the Euler equations for an ideal gas.

Experimental studies and computer simulations have also reported the presence of a uniformly fluidized state of a vibrated fluidized bed. Luding, Herrmann & Blumen (1995) carried out 'event driven' simulations of a two-dimensional system of inelastic disks in a gravitational field vibrated from below, and obtained scaling laws for the density variations in the bed. An experimental study of a vibrated fluidized bed was carried out by Warr *et al.* (1995). Their experimental set-up consisted of steel

spheres confined between two glass plates that are separated by a distance slightly larger than the diameter of the spheres. The particles were fluidized by a vibrating surface at the bottom of the bed, and the statistics of the velocity distribution of the particles were obtained using visualization techniques. Profiles for the density and the mean-square velocity were obtained, and the particle velocity distributions were also determined at certain positions in the bed. Both of these studies reported that there is an exponential dependence of the density on the height near the top of the bed, similar to the Boltzmann distribution for the density of a gas in a gravitational field. However, the dependence of the density deviates from the exponential behaviour near the bottom. The dependence of the mean-square velocity on the vibration frequency and amplitude were found to be different in the two studies.

There have been many studies on the properties of sheared suspensions which have used kinetic theory methods. The earliest attempts of Jenkins & Savage (1983) and Lun *et al.* (1984) exploited similarities between the vigorous motion of the particles in a suspension and the fluctuations of the molecules in a gas, while incorporating the difference that the collisions between the particles are inelastic, and dissipate energy. The leading-order velocity distribution was assumed to be a Maxwell–Boltzmann distribution; this assumption is valid when the energy dissipation in a collision is small compared to the energy of the particles. However, the 'temperature' of the suspension, which is proportional to the mean square of the velocity fluctuations of the particles, is determined by a balance between the source of energy due to the mean shear and the dissipation of energy due to inelastic collisions. Balance laws for the moments of the distribution function were obtained using methods similar to those used in the Chapman–Enskog theory for dense gases. Another approach is the moment expansion method, used by Jenkins & Richman (1985), where the distribution function is assumed to be an anisotropic Gaussian distribution with different mean-square velocities in different spatial directions.

The propagation of sound waves in a gas has been extensively analysed (see, for example, Sirovich & Thurber 1965; Cercignani 1975). Here, it is of interest to calculate the dispersion relation, which gives the relation between the frequency, wavelength and attenuation rate of sound in a gas. The present analysis is different from these earlier studies, because the focus is on the distribution function in the uniform state of the vibrated material. In a gas, the uniform state is determined by the thermodynamic temperature. In a dissipative granular material, the uniform state can only be maintained in the presence of external vibration, and it is of interest to study the relation between the vibration and the distribution function of the granular material. There could be oscillations superposed on the uniform state due to the vibrating surface, but the amplitude of these will be small if the frequency of oscillations of the vibrating surface is large compared to the time between successive collisions of a particle with this surface, so that there is no correlation in the velocity of the surface during successive collisions. Moreover, the experiments of Warr *et al.* (1995) did not show any systematic oscillations superposed on the uniform state, and so these oscillations are not analysed here.

In the present analysis, asymptotic techniques are used to calculate the velocity distribution function of the particles in vibro-fluidized beds in the limit where the maximum velocity of the vibrating surface is small compared to the root-mean-square velocity of the particles. In addition, the particle radius is small compared to the length scale of the density variations in the bed, which is proportional to T_0/g as discussed in the next section. In this limit it is shown, using an energy balance argument, that the dissipation of energy during a collision due to inelasticity or between successive

collisions due to viscous drag is small compared to the energy of the particles. In the leading approximation, the system is identical to a gas of hard spheres at equilibrium in a gravitational field: the density of the gas decreases exponentially away from the surface, while the temperature of the gas is independent of height. The correction to this leading-order distribution function due to dissipative effects is calculated using a moment expansion method. The perturbation to the distribution function is anisotropic with different mean-square velocities in the horizontal and vertical direction. In addition, the perturbation also has non-zero third moments of the velocity distribution function. In contrast to earlier studies on sheared suspensions, the leading-order distribution function is spatially varying at steady state, and the moments of the velocity distribution function depend on the distance from the vibrating surface. In addition, the transport of momentum and energy due to viscous and thermal effects is included in the description, in contrast to the Euler-type equations used by Goldshtein *et al.* (1995). The perturbed distribution function is inserted into the Boltzmann equation, and the equations for the moments of the distribution function are determined. The usual assumption that the particle velocities are uncorrelated before a collision (molecular chaos) is made while evaluating the collision integral. The balance equations are solved to obtain the moments of the distribution function, and the spatial variation of the density and the moments of the distribution function are determined analytically.

An issue of importance in the kinetic theory for granular materials is the appropriate form of the boundary conditions, and their relation to the mean velocity and the granular temperature at the wall, since these boundary conditions are necessary for solving the balance equations. One approach, due to Jenkins & Richman (1986), is to use microscopic models for the interaction of the particles with the wall and use averaging techniques to derive macroscopic boundary conditions. Johnson & Jackson (1987) have used a simple specularity condition at the wall to take into account the possibility of wall roughness. These types of conditions are necessary for shear flows because motion of the wall is in the tangential direction, and transmission of momentum from the particle to the wall along the tangential direction requires the presence of surface roughness. In the present case, there is a transmission of momentum in the direction normal to the wall due to the motion of the vibrating surface, and the boundary conditions can be obtained directly by considering the interaction of a particle with the wall, and averaging over the probability distributions of the particle and wall velocities.

The system analysed here consists of a vibro-fluidized bed in which the particles are confined to move in a plane. The solutions for the leading-order and the first correction to the distribution function are obtained in the next section for two cases – the first where inelastic collisions are the dominant mechanism of energy dissipation, and the second where viscous drag on the particles is the dominant dissipation mechanism. The solutions for the first correction are obtained analytically as convergent series expansions. The properties of the distribution function are discussed in §3 for the cases where inelastic collisions and viscous drag are the dominant dissipation mechanisms. In addition, the results of the present analysis are compared to the experimental results of Warr *et al.* (1995).

2. Distribution function

A Cartesian coordinate system is chosen for the analysis, where the z-direction is opposite to the direction of gravity and the x-direction is in the horizontal plane, and the particles are confined to the (x, z)-plane. The input of energy is provided by a vibrating surface located at $z = 0$. The amplitude of the vibrating surface is considered to be

small compared to the distance between successive collisions of a particle, and the frequency of vibrations is large compared to the frequency of collisions of the particles, so that the velocity of a particle colliding with the vibrating surface is uncorrelated with the velocity of the surface itself. The dynamics of the vibrating surface is described by a probability distribution $P(U)$ which is defined such that $P(U)\mathrm{d}U$ is the probability of finding the velocity of the surface in the interval $\mathrm{d}U$ about U at any time, and the mean velocity of the surface is zero. The results for the case when the mean velocity of the surface is non-zero could be very different from those for the present calculation, as discussed in Kumaran (1998). It should be noted that the present analysis is applicable to systems where the velocity of the vibrating surface varies periodically if the time period of oscillations is small compared to the time between successive collisions of particles with the surface. In this case, there is no correlation between the velocity of the surface at successive particle collisions, and consequently the dynamics of the fluidized bed is also not correlated to the frequency of the surface. It turns out that the dynamics of the system only depends on the mean-square velocity $\langle U^2 \rangle$ in the present limit where the velocity of the surface is small compared to the fluctuating velocity of the particles in the bed. For example, if the velocity of the vibrating surface is

$$U = U_0 \exp(\mathrm{i}\omega t) \tag{2.1}$$

where ω is the frequency of vibration, the probability $P(U)$ is given by

$$P(U) = \frac{1}{\pi(U_0^2 - U^2)^{1/2}} \tag{2.2}$$

and the mean-square velocity of the surface is

$$\langle U^2 \rangle = \tfrac{1}{2} U_0^2. \tag{2.3}$$

For definiteness, the above probability distribution function (2.2) will be employed in the present analysis, though the results can easily be modified to incorporate other forms of $P(U)$ as well. The system is homogeneous in the x-direction, so that the number density of the particles $\rho(z)$ is only a function of z. The velocity distribution function $f(\boldsymbol{x}, \boldsymbol{u})$ is defined such that $\rho(\boldsymbol{x}) f(\boldsymbol{x}, \boldsymbol{u})\, \mathrm{d}\boldsymbol{x}\, \mathrm{d}\boldsymbol{u}$ gives the number of particles in the differential volume $(\mathrm{d}\boldsymbol{x}\, \mathrm{d}\boldsymbol{u})$ about the point $(\boldsymbol{x}, \boldsymbol{u})$. The conservation equation for the distribution function is the steady-state Boltzmann equation

$$\frac{\partial (u_i \rho f)}{\partial x_i} + \frac{\partial (a_i \rho f)}{\partial u_i} = \frac{\partial_c (\rho f)}{\partial t}, \tag{2.4}$$

where $\boldsymbol{u}$ and $\boldsymbol{a}$ are the velocity and acceleration of the particles, the indicial notation has been used to represent vectors and a repeated index represents a dot product. The first term on the left is the convective transport of particles in real space, while the second term on the left represents the transport in velocity space due to the acceleration of the particles. The term on the right represents the rate of change of the distribution function due to the collisional transport of particles in velocity space. This is obtained by considering the collision of a particle with position and velocity $(\boldsymbol{x}, \boldsymbol{u})$ with another particle with position and velocity $(\boldsymbol{x}^\dagger, \boldsymbol{u}^\dagger)$ and integrating over the velocity of the second particle and the orientation of the line of centres at the point of collision:

$$\frac{\partial_c (\rho(\boldsymbol{x}) f(\boldsymbol{x}, \boldsymbol{u}))}{\partial t} = \rho(\boldsymbol{x}) g_0(\nu) \int \mathrm{d}\boldsymbol{u}^\dagger \int \mathrm{d}\boldsymbol{k} \rho(\boldsymbol{x}^\dagger) [f(\boldsymbol{x}', \boldsymbol{u}') f(\boldsymbol{x}^{\dagger\prime}, \boldsymbol{u}^{\dagger\prime}) - f(\boldsymbol{x}, \boldsymbol{u}) f(\boldsymbol{x}^\dagger, \boldsymbol{u}^\dagger)] (2r \boldsymbol{w} \cdot \boldsymbol{k}) \tag{2.5}$$

where $\boldsymbol{k}$ is the unit vector in the direction of the line joining the centres of the particles, $\boldsymbol{x}^{\dagger} = \boldsymbol{x} + 2r\boldsymbol{k}$, $\boldsymbol{w} = \boldsymbol{u} - \boldsymbol{u}^{\dagger}$ is the velocity difference, and the integral is carried out over all velocities such that $\boldsymbol{w}\cdot\boldsymbol{k} > 0$. The function $g_0(\nu)$ is the equilibrium radial distribution at contact, and $\nu = \rho(\boldsymbol{x})(\pi r^2)$ is the area fraction. An analytical expression for $g_0(\nu)$ has been determined by Verlet & Levesque (1982):

$$g_0(\nu) = \frac{(16 - 7\nu)}{16(1-\nu)^2}. \tag{2.6}$$

In the limit $\nu \to 0$, the above expression tends to the expected value of $g_0 = 1$, and it is in good agreement with the simulations of Hoover & Alder (1967) up to $\nu = 0.665$.

The first term in the square brackets on the right-hand side in (2.5) is the flux of particles into the differential volume about $(\boldsymbol{x}, \boldsymbol{u})$ due to collisions, and the initial velocities $(\boldsymbol{x}', \boldsymbol{u}')$ and $(\boldsymbol{x}^{\dagger\prime}, \boldsymbol{u}^{\dagger\prime})$ are chosen such that the particle at $\boldsymbol{x}$ has a final velocity $\boldsymbol{u}$ after the collision. The second term in the square bracket on the right-hand side is the flux of particles out of the differential volume about $(\boldsymbol{x}, \boldsymbol{u})$ due to collisions.

The Boltzmann equation (2.4) is a non-linear integro-differential equation, and the distribution function cannot be obtained by analytically solving this equation. However, there is an analytical solution in the following limits.

(*a*) The dissipation of energy during a collision, due to inelastic effects, or between successive collisions, due to viscous drag, is small compared to the energy of the particles. This requires that $1 - e \ll 1$ for inelastic collisions, or $\mu T_0^{1/2}/g \ll 1$ for systems where the dissipation is due to viscous drag. Here, it is assumed that the drag law is given by (2.15), and μ is the drag coefficient.

(*b*) The variation in the particle density over a distance comparable to the particle radius is small. This condition requires that $gr/T_0 \ll 1$, because the length scale for the variation of particle density is T_0/g. In this limit, it can also be shown that the correction to the radial distribution function due to variation in the particle density is small, so the pair distribution function is set equal to 1 in the leading approximation. The density of the particles scales as Ng/T_0 from equation (2.7) below, where N is the number of particles per unit length in the horizontal direction. The area fraction $\nu = \pi r^2(Ng/T_0)$, which is small because $Nr \sim 1$ and $rg/T_0 \ll 1$ in this analysis.

In this case, the system is identical to a gas of hard sphere particles under the influence of gravity, and the Boltzmann equation is identically satisfied by the following leading-order density and velocity distributions in two dimensions:

$$\rho_0 = \left(\frac{Ng}{T_0}\right)\exp\left(\frac{-gz}{T_0}\right), \tag{2.7}$$

$$f_0(\boldsymbol{x}, \boldsymbol{u}) = F(\boldsymbol{u}) = \frac{1}{2\pi T_0}\exp\left(-\frac{u_x^2 + u_z^2}{2T_0}\right), \tag{2.8}$$

where Ng/T_0 is the density at $z = 0$, N is the number of particles per unit length in the x-direction and the 'temperature' T_0 has been scaled by the mass of the particle, and has units of the square of velocity. In the leading approximation, T_0 is independent of position in the bed. An asymptotic scheme is employed in the present analysis, where the density (2.7) and distribution function (2.8) are taken as the leading-order approximations, and the effect of energy dissipation and the variation in the density over a distance comparable to the particle radius are used to calculate the higher-order corrections.

Since the temperature T_0 is independent of position in the leading approximation, it can be determined by a macroscopic energy balance over the entire bed. There

is a source of energy due to particle collisions with the vibrating surface at $z = 0$, and dissipation due to inelastic collisions and the drag force due to the gas. The leading-order temperature and density are calculated by balancing the leading-order contributions to the source and dissipation of energy.

The source of momentum and energy at the vibrating surface is determined by analysing the collisions between the particles and the surface. The particle–base collisions are considered to be elastic in the present case, but the analysis can easily be extended to inelastic collisions as well. The variation in the height of the surface is neglected since this is small compared to the mean free path of the particles, and only the variation in the velocity is included in the analysis of the collisions. The frequency of a collision between a particle of velocity $\boldsymbol{u}$ and the surface (per unit length of the surface) is $(Ng/T_0)(U-u_z)f(0,\boldsymbol{u})$. The velocity of a particle after an inelastic collision is $u_z' = 2U - u_z$, and the change in energy is $(1/2)(u_z'^2 - u_z^2) = 2U(U-u_z)$. (Note that the momentum and energy have been scaled by the mass of the particle in a manner similar to the temperature.) Therefore, the total change in energy per unit width of the surface per unit time due to particle collisions with the vibrating surface is

$$S = \int_{-U_0}^{U_0} \mathrm{d}U \int_{-\infty}^{U} \mathrm{d}u_z P(U) \frac{Ng}{T_0} f(0,\boldsymbol{u}) 2U(U-u_z)^2, \tag{2.9}$$

where the limits of integration are chosen so that $U - u_z > 0$. While determining the leading-order contribution to S, it is sufficient to consider the leading-order contribution to the distribution function $f(0,\boldsymbol{u}) = F(\boldsymbol{u})$ in (2.9). The integral in (2.9) is difficult to evaluate even with this simplification, but it is possible to obtain a series solution in the small parameter U_0^2/T in the limit $U_0^2 \ll T$. In this limit, the leading-order contribution to the source of energy S_0 is

$$S_0 = \left(\frac{2}{\pi}\right)^{1/2} \frac{Ng}{T_0^{1/2}} U_0^2. \tag{2.10}$$

For a suspension where the dissipation of energy is due to inelastic collisions, the rate of energy dissipation is

$$D_I = -\int_0^{\infty} \mathrm{d}z \rho(z) \rho(z^{\dagger}) g_0(v) \int \mathrm{d}\boldsymbol{u} \int \mathrm{d}\boldsymbol{u}^{\dagger} \int \mathrm{d}\boldsymbol{k} f(\boldsymbol{x},\boldsymbol{u}) f(\boldsymbol{x}^{\dagger},\boldsymbol{u}^{\dagger}) (2r\boldsymbol{w}\cdot\boldsymbol{k})(u'^2 - u^2)/2 \tag{2.11}$$

where u and u' are the magnitudes of the particle velocities after and before a collision, $\boldsymbol{k}$ is the unit vector in the direction of the line joining the centres of the particles at the point of collision and $\boldsymbol{w} = \boldsymbol{u} - \boldsymbol{u}^{\dagger}$. Note that there is a negative sign in (2.11) because the dissipation rate is the negative of the rate of change of energy of the suspension. In determining the leading-order estimate D_{I0}, the variation in the density over a distance comparable to the particle radius is neglected, the radial distribution function g_0 is set equal to 1 and the leading-order energy dissipation rate is

$$D_{I0} = \pi^{1/2} r N^2 g T_0^{1/2} (1 - e^2). \tag{2.12}$$

Equating the leading-order source of energy due to the vibrating surface and the energy dissipation, the leading-order temperature is

$$T_0 = \frac{\sqrt{2}}{\pi} \frac{U_0^2}{rN(1-e^2)}. \tag{2.13}$$

In the perturbation analysis of a system where the dissipation is due to inelastic

collisions, the small parameter ϵ is defined as

$$\epsilon_I = \frac{U_0^2}{T_0} = \frac{\pi}{\sqrt{2}} rN(1-e^2). \tag{2.14}$$

This parameter is independent of the amplitude of the velocity of the vibrating surface, and depends only on the number of layers of particles and the radius and coefficient of restitution of the particles.

For analysing the effect of viscous dissipation, a drag law is considered to be of the form

$$a_i = -\mu u_i \tag{2.15}$$

where μ is the drag coefficient. The dissipation of energy due to the drag force is

$$D_D = \int_0^\infty \rho(z) \int \mathrm{d}\boldsymbol{u} f(\boldsymbol{x},\boldsymbol{u}) \mu(\boldsymbol{u}\cdot\boldsymbol{u}). \tag{2.16}$$

The leading-order contribution D_{D0} to the dissipation due to viscous drag can be evaluated by substituting $F(\boldsymbol{u})$ for $f(\boldsymbol{x},\boldsymbol{u})$ and $\rho_0(z)$ for $\rho(z)$ in the above expression:

$$D_{D0} = 2\mu N T_0, \tag{2.17}$$

and the leading-order temperature is obtained by equating D_{D0} and S_0:

$$T_0 = \left(\frac{1}{(2\pi)^{1/2}} \frac{U_0^2 g}{\mu} \right)^{2/3}. \tag{2.18}$$

In this case, the parameter ϵ is defined as

$$\epsilon_D = \frac{U_0^2}{T_0} = \left(\frac{(2\pi)^{1/2}\mu U_0}{g} \right)^{2/3} = \left(\frac{(2\pi)^{1/2}\mu T_0^{1/2}}{g} \right). \tag{2.19}$$

This parameter now depends on the amplitude of the velocity oscillation of the surface. In the present analysis we consider the limit where $\epsilon = U_0^2/T_0 \ll 1$, and use a perturbation analysis to determine the properties of the system. This parameter assumes different values for situations where the dissipation of energy is due to inelastic collisions and due to the viscous drag force. However, it provides a unified framework for the formulation of the equations of motion, and a distinction between the two mechanisms is made only when the results for the variation in the density and the velocity moments are calculated.

The dissipation of energy causes a small correction to the density $\rho = \rho_0(z)(1 + \epsilon\rho_1(z))$, a correction to the temperature $T = T_0(1 + \epsilon T_1(z))$, and a perturbation to the form of the distribution function which is assumed to be of the form

$$\begin{aligned} f(\boldsymbol{x},\boldsymbol{u}) = F(\boldsymbol{u}) \Bigg[1 + \epsilon \Bigg(& \frac{T_1(z)(u_x^2 + u_z^2 - 2T_0)}{2T_0} + \frac{A_1(z)u_z}{T_0^{1/2}} \\ & + \frac{A_2(z)(u_z^2 - u_x^2)}{T_0} + \frac{A_3(z)u_z^3}{T_0^{3/2}} - \frac{(A_1(z) + 3A_3(z))u_x^2 u_z}{T_0^{3/2}} \Bigg) \Bigg] \\ = F(\boldsymbol{u})(1 + \epsilon\Phi(\boldsymbol{x},\boldsymbol{u})). & \end{aligned} \tag{2.20}$$

The terms in the perturbation expansion are suitably scaled by different powers of the temperature T_0 so that T_1, A_1, A_2 and A_3 are dimensionless. The term proportional to T_1 in the above represents the variation in the distribution function due to the

variation in the temperature, while the other terms are chosen so that the variation in the form of the distribution function does not alter the temperature. In addition, the term proportional to u_z^3 has been chosen so that the mean velocity in the z-direction is zero at all points.

The functions ρ_1, T_1, A_1, A_2 and A_3 are determined using the moment expansion method. Conservation equations for the moments of the velocity distribution function are determined by multiplying the Boltzmann equation by products of the components of the particle velocity and integrating over velocity space. The moment $\langle\psi(\boldsymbol{x})\rangle$ of a function $\psi(\boldsymbol{u})$ of the particle velocity is

$$\langle\psi(\boldsymbol{x})\rangle = \int \mathrm{d}\boldsymbol{u}\psi(\boldsymbol{u})f(\boldsymbol{x},\boldsymbol{u}). \tag{2.21}$$

Equations for five functions of the velocity distribution, u_z, u_z^2, u_x^2, u_z^3 and $u_x^2u_z$, are considered in the present analysis. The moments of these functions can be expressed in terms of the functions T_1, A_1, A_2 and A_3:

$$\langle u_z\rangle = 0, \tag{2.22}$$

$$\langle u_z^2\rangle = T_0 + \epsilon T_0(T_1 + 2A_2), \tag{2.23}$$

$$\langle u_x^2\rangle = T_0 + \epsilon T_0(T_1 - 2A_2), \tag{2.24}$$

$$\langle u_z^3\rangle = 6\epsilon T_0^{3/2}A_3, \tag{2.25}$$

$$\langle u_x^2u_z\rangle = -2\epsilon T_0^{3/2}(A_1 + 3A_3). \tag{2.26}$$

The conservation equations for the above moments are

$$\partial_z(\rho\langle u_z^2\rangle) + g\rho = \frac{\partial_c\rho\langle u_z\rangle}{\partial t}, \tag{2.27}$$

$$\partial_z(\rho\langle u_z^3\rangle) + 2\mu\rho\langle u_z^2\rangle = \frac{\partial_c\rho\langle u_z^2\rangle}{\partial t}, \tag{2.28}$$

$$\partial_z(\rho\langle u_x^2u_z\rangle) + 2\mu\rho\langle u_x^2\rangle = \frac{\partial_c\rho\langle u_x^2\rangle}{\partial t}, \tag{2.29}$$

$$\partial_z(\rho\langle u_z^4\rangle) + 3g\rho\langle u_z^2\rangle + 3\mu\rho\langle u_z^3\rangle = \frac{\partial_c\rho\langle u_z^3\rangle}{\partial t}, \tag{2.30}$$

$$\partial_z(\rho\langle u_x^2u_z^2\rangle) + g\rho\langle u_x^2\rangle + \mu\rho\langle u_x^2u_z\rangle = \frac{\partial_c\rho\langle u_x^2u_z\rangle}{\partial t}. \tag{2.31}$$

The rate of change of a moment $\psi(\boldsymbol{x})$ due to particle collision is obtained by considering a collision between two particles with positions z and $z^\dagger$, initial velocities $\boldsymbol{u}$ and $\boldsymbol{u}^\dagger$, and with final velocities $\boldsymbol{u}'$ and $\boldsymbol{u}^{\dagger\prime}$, and integrating over all $\boldsymbol{u}$ and $\boldsymbol{u}^\dagger$:

$$\frac{\partial_c\rho\langle\psi_i(\boldsymbol{x})\rangle}{\partial t} = \rho(z)\rho(z^*)\int \mathrm{d}\boldsymbol{u}\int \mathrm{d}\boldsymbol{u}^\dagger\int \mathrm{d}\boldsymbol{k}f(\boldsymbol{x},\boldsymbol{u})f(\boldsymbol{x}^\dagger,\boldsymbol{u}^\dagger)(\psi(\boldsymbol{u}') - \psi(\boldsymbol{u}))(2r\boldsymbol{w}\cdot\boldsymbol{k}). \tag{2.32}$$

It is useful to briefly describe the method used for evaluating the collision integrals. The velocities of the two particles before the collision are separated into the velocity of the centre of mass $\boldsymbol{v}$ and the velocity difference between the two particles $\boldsymbol{w}$ as follows:

$$v_i = (u_i + u_i^\dagger)/2, \quad w_i = u_i - u_i^\dagger. \tag{2.33}$$

The centre-of-mass velocity after the collision is equal to the centre-of-mass velocity before the collision, while the velocity difference between the two particles after the

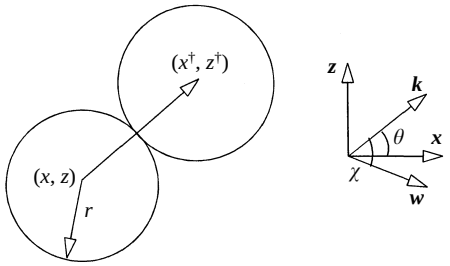

FIGURE 1. Coordinate system for analysing collisions between particles.

collision is given by

$$w_i' = (\delta_{ij} - (1+e)k_i k_j)w_j, \tag{2.34}$$

where the vector $\boldsymbol{k}$ is the unit vector joining the centres of the two disks and δ_{ij} is the identity tensor. With these substitutions, (2.32) can be expressed as an integral over the velocities $\boldsymbol{v}$ and $\boldsymbol{w}$:

$$\frac{\partial_c \rho\langle\psi_i(\boldsymbol{x})\rangle}{\partial t} = \rho(z)\rho(z^\dagger)\int \mathrm{d}\boldsymbol{v}\int \mathrm{d}\boldsymbol{w}\int \mathrm{d}\boldsymbol{k}F(\boldsymbol{v})F(\boldsymbol{w})(1+\epsilon(\Phi(\boldsymbol{x},\boldsymbol{u})+\Phi(\boldsymbol{x}^\dagger,\boldsymbol{u}^\dagger)) \times(\psi(\boldsymbol{u}')-\psi(\boldsymbol{u}))(2rw_i k_i), \tag{2.35}$$

where $F(\boldsymbol{v}) = (\pi T_0)^{-1}\exp(-v^2/T_0)$ and $F(\boldsymbol{w}) = (4\pi T_0)^{-1}\exp(-w^2/4T_0)$ are the leading-order distribution functions for the velocity of the centre of mass and the difference velocity. In (2.35), only the $O(\epsilon)$ corrections to the distribution function have been included in the calculation, since the collision integrals are evaluated correct to $O(\epsilon)$. The integral over the velocity $\boldsymbol{v}$ can easily be evaluated, since it is decoupled from the other two integrals. The configuration shown in figure 1 is used to evaluate the integrals over $\boldsymbol{k}$ and $\boldsymbol{w}$. The vector $\boldsymbol{k}$ makes an angle θ with the vertical, while the vector $\boldsymbol{w}$ makes an angle χ with $\boldsymbol{k}$. The components of $\boldsymbol{w}$ can be expressed in terms of θ and χ:

$$\left.\begin{aligned} w_x &= w(\cos(\chi)\cos(\theta) - \sin(\chi)\sin(\theta)),\\ w_z &= w(\sin(\chi)\cos(\theta) + \cos(\chi)\sin(\theta)),\\ w_x' &= w(-e\cos(\chi)\cos(\theta) - \sin(\chi)\sin(\theta)),\\ w_z' &= w(-e\cos(\chi)\sin(\theta) + \sin(\chi)\cos(\theta)). \end{aligned}\right\} \tag{2.36}$$

The collisional rate of change of the function ψ can now be expressed in terms of w, χ and θ as

$$\frac{\partial_c \rho\langle\psi_i(\boldsymbol{x})\rangle}{\partial t} = \rho(z)\rho(z^\dagger)g_0(\nu)\int \mathrm{d}\boldsymbol{v}\int_0^\infty w\,\mathrm{d}w\int_0^{2\pi}\mathrm{d}\theta\int_{-\pi/2}^{\pi/2}\mathrm{d}\chi F(\boldsymbol{v})F(\boldsymbol{w}) \times(1+\epsilon(\Phi(\boldsymbol{x},\boldsymbol{u})+\Phi(\boldsymbol{x}^\dagger,\boldsymbol{u}^\dagger))(\psi(\boldsymbol{u}')-\psi(\boldsymbol{u}))(2rw\cos\chi), \tag{2.37}$$

where $\Phi(\boldsymbol{x},\boldsymbol{u})$ is defined in (2.20) Note that the angle χ has been integrated between $(-\pi/2)$ and $(\pi/2)$ because the two particles collide only for $-\pi/2 \leqslant \chi \leqslant \pi/2$ where $(\boldsymbol{w}\cdot\boldsymbol{k})$ is positive.

In the limit $\epsilon \ll 1$, the conservation equations are identically satisfied in the leading-order approximation by the Boltzmann distribution, while the $O(\epsilon)$ corrections to the equations are solved to obtain the functions ρ_1, T_1, A_1, A_2 and A_3. It is convenient to express the equations in terms of a scaled length $z^* = zg/T_0$, a scaled velocity $u_i^* = u_i/T_0^{1/2}$, and a scaled density $\rho_0^* = \rho_0 T_0/Ng = \exp(-z^*)$. The scaled equations

for the $O(\epsilon)$ correction to the conservation equations are

$$\epsilon[d_{z^*}(\rho_0^*(T_1+2A_2+\rho_1))+\rho_0^*\rho_1] = \left.\frac{\partial_c\rho_0^*\langle u_z^*\rangle}{\partial t^*}\right|_1, \tag{2.38}$$

$$\epsilon[d_{z^*}(6\rho_0^*A_3)]+\left(\frac{2}{\pi}\right)^{1/2}\rho_0^*\epsilon_D = \left.\frac{\partial_c\rho_0^*\langle u_z^{*2}\rangle}{\partial t^*}\right|_1, \tag{2.39}$$

$$\epsilon[d_{z^*}(-2\rho_0^*(A_1+3A_3))]+\left(\frac{2}{\pi}\right)^{1/2}\rho_0^*\epsilon_D = \left.\frac{\partial_c\rho_0^*\langle u_x^{*2}\rangle}{\partial t^*}\right|_1, \tag{2.40}$$

$$\epsilon[d_{z^*}(3\rho_0^*(2T_1+4A_2+\rho_1))+3\rho_0^*(\rho_1+T_1+2A_2)] = \left.\frac{\partial_c\rho_0^*\langle u_z^{*3}\rangle}{\partial t^*}\right|_1, \tag{2.41}$$

$$\epsilon[d_{z^*}(\rho_0^*(2T_1+\rho_1))+\rho_0^*(T_1-2A_2+\rho_1)] = \left.\frac{\partial_c\rho_0^*\langle u_z^*u_x^{*2}\rangle}{\partial t^*}\right|_1. \tag{2.42}$$

In the leading-order approximation, the collisional change in the velocity moments is identically zero, since the Boltzmann equation is identically satisfied by the distribution function. The first correction to the collisional rate of change of the velocity moments is due to the following four factors.

(*a*) The perturbation to the distribution function (2.20). While calculating this effect, the collisions can be considered elastic, the variation in the density over a length comparable to the particle size can be neglected, and the deviation in the radial distribution function from its value of 1 in the dilute limit is neglected since the inclusion of these effects causes subdominant corrections in the asymptotic scheme. With this approximation, the rates of change of the velocity moments due to the perturbation to the distribution function, scaled in a manner similar to the balance equations (2.38)–(2.42) are

$$\frac{\partial_p(\rho_0^*\langle u_z^*\rangle)}{\partial t^*} = 0, \tag{2.43}$$

$$\frac{\partial_p(\rho_0^*\langle u_z^{*2}\rangle)}{\partial t^*} = -8\pi^{1/2}\epsilon A_2(Nr)\rho_0^{*2}, \tag{2.44}$$

$$\frac{\partial_p(\rho_0^*\langle u_x^{*2}\rangle)}{\partial t^*} = 8\pi^{1/2}\epsilon A_2(Nr)\rho_0^{*2}, \tag{2.45}$$

$$\frac{\partial_p(\rho_0^*\langle u_z^{*3}\rangle)}{\partial t^*} = 6\pi^{1/2}\epsilon(-A_1-6A_3)(Nr)\rho_0^{*2}, \tag{2.46}$$

$$\frac{\partial_p(\rho_0^*\langle u_z^*u_x^{*2}\rangle)}{\partial t^*} = 2\pi^{1/2}\epsilon(5A_1+18A_3)(Nr)\rho_0^{*2}. \tag{2.47}$$

(*b*) There is a correction to the distribution function due to the inelastic nature of the collisions. While calculating the leading-order effect of inelastic collisions, the perturbation to the distribution function and the effect of variation in density on the collision integral are neglected, the pair distribution function is set equal to its value of 1 in the dilute limit, and the rates of change of the velocity moments due to inelastic collisions are

$$\frac{\partial_i(\rho_0^*\langle u_z^*\rangle)}{\partial t^*} = 0, \tag{2.48}$$

$$\frac{\partial_i(\rho_0^*\langle u_z^{*2}\rangle)}{\partial t^*} = -2\left(\frac{2}{\pi}\right)^{1/2}\epsilon_I\rho_0^{*2}, \tag{2.49}$$

$$\frac{\partial_i(\rho_0^*\langle u_x^{*2}\rangle)}{\partial t^*} = -2\left(\frac{2}{\pi}\right)^{1/2}\epsilon_I\rho_0^{*2}, \tag{2.50}$$

$$\frac{\partial_i(\rho_0^*\langle u_z^{*3}\rangle)}{\partial t^*} = 0, \tag{2.51}$$

$$\frac{\partial_i(\rho_0^*\langle u_z^* u_x^{*2}\rangle)}{\partial t^*} = 0. \tag{2.52}$$

(*c*) There is a variation in the collision integral due to the variation in the density over distances of the order of the particle radius. The effect of the density variation is proportional to the small parameter $\epsilon_G = (rg/T_0)$, which is the ratio of the particle radius and the length scale of the variation of properties in the fluidized bed. The leading-order effect due to this is determined using a Taylor series expansion for the leading-order density:

$$\begin{aligned}\rho_0(z^*) &= \rho_0(z) + (z^* - z)\partial_z\rho_0(z) \\ &= \rho_0(z)\left(1 - \frac{(z^* - z)g}{T_0}\right).\end{aligned} \tag{2.53}$$

With this approximation, the contribution to the collisional rates of change of the velocity moments due to the gradients in the density are

$$\frac{\partial_g(\rho_0^*\langle u_z^*\rangle)}{\partial t^*} = 4\pi\epsilon_G(rN)\rho_0^{*2}, \tag{2.54}$$

$$\frac{\partial_g(\rho_0^*\langle u_z^{*2}\rangle)}{\partial t^*} = 0, \tag{2.55}$$

$$\frac{\partial_g(\rho_0^*\langle u_x^{*2}\rangle)}{\partial t^*} = 0, \tag{2.56}$$

$$\frac{\partial_g(\rho_0^*\langle u_z^{*3}\rangle)}{\partial t^*} = 12\pi\epsilon_G(rN)\rho_0^{*2}, \tag{2.57}$$

$$\frac{\partial_g(\rho_0^*\langle u_x^{*2}u_z^*\rangle)}{\partial t^*} = 4\pi\epsilon_G(rN)\rho_0^{*2}. \tag{2.58}$$

While calculating the above correction, the effect of inelasticity and the variation in the distribution function from the Maxwell–Boltzmann distribution are neglected, and the pair distribution function is set equal to its value of 1 in the dilute limit.

(*d*) The effect of variation in the pair distribution function due to variations in the density. The pair distribution function (2.6) can be expanded in a Taylor series in the area fraction $v = \rho\pi r^2$. In the leading approximation, $v = (Nr)\epsilon_G\exp(-z^*)$, and the pair distribution function is given by $g_0(v) = 1 + (25/16)(Nr)\epsilon_G\exp(-z^*)$ correct to $O(\epsilon_G)$. As anticipated earlier, the correction to the pair distribution function due to variations in the particle density is $O(\epsilon_G)$. The $O(\epsilon)$ correction to the collisional change in the velocity moments can be obtained by including the correction to the radial distribution function, but neglecting the corrections due to inelasticity, the deviation in the distribution function from the Maxwell–Boltzmann distribution and the variation in the density over a distance equal to the particle radius. In this case, it can easily be verified that the $O(\epsilon_G)$ correction to the collisional terms is identically zero. This is because the collisional corrections are just equal to the $O(\epsilon_G)$ correction to the radial distribution function times the leading-order collisional changes in the velocity moments, and the latter are identically zero. Consequently, the $O(\epsilon_G)$ correction due to deviation in the value of the radial distribution function from its value of 1 in the dilute limit is zero in the present asymptotic scheme.

The boundary conditions for the solutions of equations (2.38)–(2.42) are obtained as follows. The condition for ρ_1 is obtained by stipulating that a variation in the density does not alter the total number of particles in the suspension. This requires that

$$\int_0^\infty \mathrm{d}z^* \exp(-z^*)\rho_1(z^*) = 0. \tag{2.59}$$

The condition for T_1 is obtained from energy balance conditions for the entire bed, in a manner similar to that used for obtaining the temperature T_0 in the leading approximation

$$S_1 = D_1 \tag{2.60}$$

where D_1 is the $O(\epsilon)$ correction to the dissipation of energy, and S_1 is the $O(\epsilon)$ correction to the source of energy at the vibrating surface. The $O(\epsilon)$ correction to the energy source at the surface, obtained in a manner analogous to S_0 (2.10), is

$$S_1 = \epsilon^2 N g T_0^{1/2} \left(\frac{1}{4(2\pi)^{1/2}} + \frac{1}{(2\pi)^{1/2}}(2A_2 + T_1) + \left(\frac{2}{\pi}\right)^{1/2} \rho_1 \right). \tag{2.61}$$

For a system where the energy dissipation is due to inelastic collisions, the $O(\epsilon)$ correction to the energy dissipation due to inelastic collisions, obtained in a manner similar to D_{I0} (2.12), is

$$D_{I1} = \epsilon_I^2 N g T_0^{1/2} \left(\frac{2}{\pi}\right)^{1/2} \left(\int_0^\infty \mathrm{d}z^* \exp(-2z^*)(3T_1 + 4\rho_1) \right). \tag{2.62}$$

For a system where the energy dissipation is due to viscous drag, the $O(\epsilon^2)$ correction to the energy dissipation is

$$D_{D1} = \left(\frac{2}{\pi}\right)^{1/2} \epsilon_D^2 N g T_0^{1/2} \int_0^\infty \mathrm{d}z^* \exp(-z^*)(T_1 + \rho_1). \tag{2.63}$$

The condition for the first correction to the temperature T_1 is obtained by equating the source of energy (2.61) to the dissipation of energy (2.62) or (2.63). The boundary conditions for the functions A_1 and A_3 are determined from the requirement that the flux of the moments $\langle u_z^{*2} \rangle$ and $\langle u_x^{*2} \rangle$ due to the vibrating surface is identical to that obtained from the perturbed distribution function. The fluxes of the velocity moments are evaluated using a procedure similar to that used for the flux of energy from the vibrating surface (2.9). The flux of $\langle u_x^2 \rangle$ at the vibrating surface is identically zero, because there is no change in the tangential velocity of the particles due to collisions with the surface. This condition results in the following boundary condition at $z = 0$:

$$(A_1 + 3A_3)|_{z=0} = 0. \tag{2.64}$$

The leading-order contribution to the flux of $\langle u_z^{*2} \rangle$ at the surface is

$$\rho_0^* \langle u_z^3 \rangle = 2 \left(\frac{2}{\pi}\right)^{1/2} T_0^{1/2} U_0^2. \tag{2.65}$$

From this, the following condition for $A_1(z)$ is obtained:

$$A_1(z)|_{z=0} = -\left(\frac{2}{\pi}\right)^{1/2}. \tag{2.66}$$

3. Results

3.1. *Dissipation due to inelastic collisions*

A suspension in which the dissipation is due to inelastic collisions is considered first. An equation for $A_1(z^*)$ is obtained by adding ((2.39) and (2.40)), and this is solved to obtain:

$$A_1(z) = -\left(\frac{2}{\pi}\right)^{1/2} \exp(-z^*). \tag{3.1}$$

In the above solution, an exponentially growing term has been neglected due to the constraint that A_1 is finite at large z^*, and it can easily be verified that the above solution is consistent with the boundary condition (2.66).

A differential equation for A_2 can be obtained by taking (2.41) $-3\times$ (2.42), and using the appropriate collisional terms:

$$d_z A_2(z) = -3\pi^{1/2}(Nr)(A_1 + 4A_3)\rho_0^*. \tag{3.2}$$

Taking a derivative of this with respect to z and using (2.39) and (2.40) for the derivatives $d_{z^*}(\rho_0^* A_1)$ and $d_{z^*}(\rho_0^* A_3)$, the following second-order differential equation is obtained for $A_2(z)$:

$$d_z^2 A_2(z) = \left[16\pi A_2(Nr) - 2\sqrt{2}\right](Nr)\exp(-2z^*). \tag{3.3}$$

The above equation cannot be solved analytically, but a series solution in the parameter $\exp(-2z^*)$ can be obtained for $z^* \gg 1$. In this limit, there are two leading-order solutions for A_2; one solution is independent of z^* and the other is a linear function of z^*. The latter is not finite in the limit $z^* \gg 1$, and is neglected. With this simplification, the series solution for z^* is

$$A_2(z^*) = \sum_{n=0}^{\infty} A_{2n}\exp(-2nz^*), \quad A_{21} = \left[4\pi(Nr)^2 A_{20} - \frac{(Nr)}{\sqrt{2}}\right], \quad A_{2n} = \frac{4\pi(Nr)^2 A_{2(n-1)}}{n^2}, \tag{3.4}$$

where A_{20} is a constant of integration determined using the boundary conditions. The above series is convergent even in the limit $z^* \to 0$, because the ratio $A_{2(n+1)}/A_{2n} \sim (4\pi Nr)/n^2$ for $n \gg 1$, and the above series solution provides a uniform approximation in the range $0 \leqslant z^* \leqslant \infty$. The function $A_3(z)$ can be determined from the balance equation (2.40) and the solution (3.4) for $A_2(z^*)$:

$$A_3(z^*) = \frac{2\pi^{1/2}(Nr)}{3}\sum_{n=0}^{\infty}\frac{A_{2n}\exp[-(2n+1)z^*]}{(n+1)} + \frac{1}{6}\left(\frac{2}{\pi}\right)^{1/2}\exp(-z^*). \tag{3.5}$$

In the above equation, the constant of integration has been set equal to zero due to the constraint that A_3 is finite in the limit $z^* \to \infty$. The constant of integration A_{20} can be determined by inserting the solutions (3.1) and (3.5) for $A_1(z^*)$ and $A_3(z^*)$ into the boundary condition (2.66). It can easily be seen from the differential equations and the boundary conditions that $A_1(z^*)$, $A_2(z^*)$ and $A_3(z^*)$ are independent of the parameter ϵ_G.

A differential equation for T_1 is obtained by taking (2.41) $-3\times$ (2.38), and taking the derivative with respect to z^* of the resulting equation:

$$d_{z^*}^2(T_1 + 2A_2) = \left[16\pi A_2(Nr) + 4\left(\frac{2}{\pi}\right)^{1/2}\right]\exp(-2z^*). \tag{3.6}$$

The series solution for the above equation is obtained using the solution (3.4) for $A_2(z^*)$:

$$T_1 = T_{10} + \sum_{n=0}^{\infty} \left[\frac{4\pi (Nr)^2 A_{2n} \exp[-2(n+1)z^*]}{(n+1)^2} - 2A_{2n} \exp(-2nz^*) \right] \tag{3.7}$$

where T_{10} is an unknown constant to be determined from the boundary conditions. The first correction to the density ρ_1 can be determined from (2.38), using the solutions (3.4) and (3.7) for $A_2(z^*)$ and $T_1(z^*)$:

$$\rho_1 = \rho_{10} + T_{10} z^* - 4\pi \epsilon_G (Nr) \exp(-z^*) + \sum_{n=1}^{\infty} \left[\frac{-(2n+1)}{2n} (T_{1n} + 2A_{2n}) \exp(-2nz^*) \right]. \tag{3.8}$$

The solutions (3.7) and (3.8) for the functions ρ_1 and T_1 contain two unknown constants, T_{10} and ρ_{10}, which are determined using the integral balance conditions (2.59) and (2.60), where the first correction to the dissipation rate is given by (2.62). The solutions (3.1), (3.4), (3.5), (3.7) and (3.8) for $A_1(z^*), A_2(z^*), A_3(z^*), T_1(z^*)$ and $\rho_1(z^*)$ can be used to determine the $O(\epsilon_I)$ correction to the velocity moments given in (2.22)–(2.26).

The leading-order contribution to the anisotropy in the mean-square velocity, $(\langle u_z^{*2} - u_x^{*2} \rangle) = 4A_2(z^*)$, is shown as a function of z^* in figure 2(*a*) for three different values of (Nr). As explained earlier, the function $A_2(z^*)$ is independent of ϵ_G, and so the leading-order contribution to the difference in the mean-square velocities is also independent of ϵ_G. From figure 2(*a*), it is seen that the mean-square velocity in the vertical direction is always larger than that in the horizontal direction. The difference between the two decreases with increasing z^*, and attains a constant value in the limit $z^* \to \infty$, and this limiting value is proportional to $(Nr)^{-1}$. The value of the anisotropy is determined by a balance between the collisional transport of energy from the horizontal to the vertical velocity fluctuations and the dissipation of energy due to inelastic collisions. Both of these decrease proportional to ρ_0^{*2} in the limit $\rho_0^* \ll 1$ (see (2.44), (2.45), (2.49) and (2.50)), and the anisotropy attains a constant value in this limit. In addition, the rate of transport of energy is proportional to $A_2(Nr)$ from (2.44) and (2.45), while the rate of dissipation of energy is independent of (Nr), and consequently the value of the anisotropy in the limit $z^* \to 0$ is proportional to $(Nr)^{-1}$.

The $O(\epsilon_I)$ corrections to the third moments of the velocity distribution, $\langle u_z^{*3} \rangle$ and $\langle u_x^{*2} u_z^* \rangle$, are shown as a function of z^* in figures 2(*b*) and 2(*c*). The first correction to the third moments are functions of $A_1(z^*)$ and $A_3(z^*)$ (see (2.25) and (2.26)), and are independent of ϵ_G for reasons provided earlier. The figure 2(*b*) shows that $\langle u_z^{*3} \rangle$ decreases as z^* increases, and has a limiting behaviour proportional to $\exp(-z^*)$ in the limit $z^* \to \infty$. In addition, this limiting value shows a very weak dependence on Nr. These qualitative features can be explained as follows. Equation (2.28) indicates that the conduction of energy in the vertical direction is due to a gradient in $\rho_0^* \langle u_z^{*3} \rangle$, while the dissipation of energy due to inelastic collisions is proportional to ρ_0^{*2}. A balance between these two provides the behaviour $\langle u_z^{*3} \rangle \propto \exp(-z^*)$, and the weak dependence of $\langle u_z^{*3} \rangle$ on Nr. The figure 2(*c*) shows that the velocity moment $\langle u_x^{*2} u_z^* \rangle$ first increases and then decreases with increasing z^*, and shows a behaviour similar to $\langle u_z^{*3} \rangle$ in the limit $z^* \to \infty$. The initial increase in $\langle u_x^{*2} u_z^* \rangle$ is due to the boundary condition (2.64), which stipulates that $\langle u_x^{*2} u_z^* \rangle = 0$ at $z^* = 0$, while the reasons for the qualitative trends in the limit $z^* \to \infty$ are identical to those for the behaviour of $\langle u_z^{*3} \rangle$.

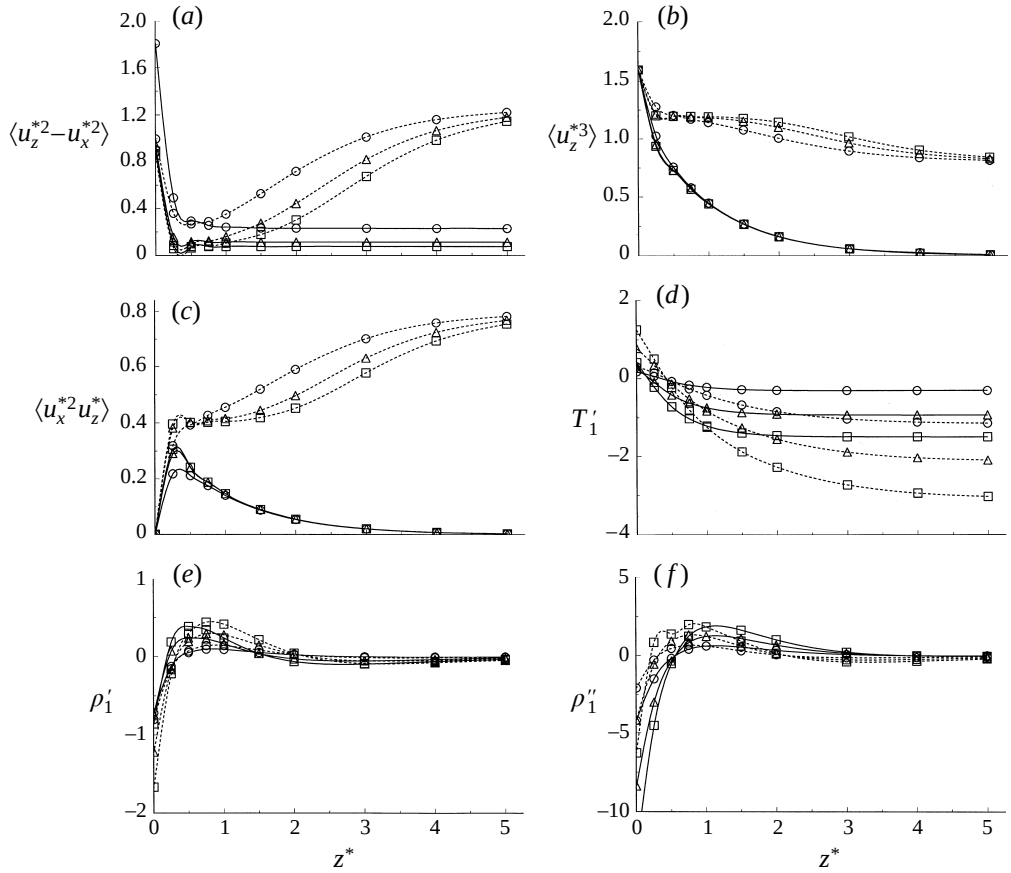

FIGURE 2. Properties of the velocity distribution function: (*a*) the scaled anisotropy $\langle u_z^{*2} - u_x^{*2} \rangle$; (*b*) the third moment $\langle u_z^{*3} \rangle$; (*c*) the third moment $\langle u_x^{*2} u_x^{*} \rangle$; (*d*) the function T_1'; (*e*) the function ρ_1'; (*f*) the function ρ_1'', all as a function of the scaled vertical coordinate z^*. The solid lines are for a system where inelastic collision is the dominant dissipation mechanism, and the broken lines are for a system where viscous drag is the dominant dissipation mechanism. ○, $Nr = 1.0$; △, $Nr = 2.0$; □, $Nr = 3.0$.

The first corrections to the temperature and density, $T_1(z^*)$ and $\rho_0(z^*)\rho_1(z^*)$, are functions of the parameter ϵ_G which accounts for the leading-order correction due to variations in the concentration field over distances comparable to the particle diameter. These can be expressed as $T_1 = T_1' + (\epsilon_G/\epsilon_I)T_1''$ and $(\rho_0\rho_1) = \rho_1'(z^*) + (\epsilon_G/\epsilon_I)\rho_1''(z^*)$. It turns out that the function $T_1'' = -2.0944(Nr)$ is independent of z^*, and the functions T_1', ρ_1' and ρ_1'' are shown as functions of z^* in figures 2(*d*), 2(*e*) and 2(*f*). It is observed that T_1' is positive for small z^*, decreases as z^* is increased and attains a constant negative value in the limit $z^* \to \infty$. An opposite trend is observed for the functions $\rho_1'(z^*)$ and $\rho_1''(z^*)$, which are negative for small z^*, increase and assume positive values for intermediate values of z^* and then decrease proportional to $z^* \exp(-z^*)$ in the limit $z^* \to \infty$. It is useful to note that the functions T_1'' and ρ_1'' are larger than T_1' and ρ_1', indicating that the effect of variation in the gradients in the concentration field on collisional interactions dominates the effect of the perturbation to the distribution function for $(\epsilon_G/\epsilon_I) \sim 1$.

3.2. *Dissipation due to viscous drag*

The functions A_1, A_2, A_3, ρ_1 and T_1 for a suspension where viscous dissipation is the dominant mechanism of dissipation is considered next. The method of analysis is identical to the case where the dissipation is due to inelastic collisions, so the details are not provided, and the final results are

$$A_1(z^*) = -\left(\frac{2}{\pi}\right)^{1/2}, \tag{3.9}$$

$$\left.\begin{aligned} A_2(z^*) &= \sum_{n=0}^{\infty} A_{2n} \exp(-nz^*), \\ A_{21} &= -\sqrt{2}(Nr), \\ A_{2n} &= \frac{16\pi(Nr)^2 A_{2(n-2)}}{n^2} \quad \text{for} \quad n \geqslant 2, \end{aligned}\right\} \tag{3.10}$$

$$A_3(z^*) = \frac{1}{6}\left(\frac{2}{\pi}\right)^{1/2} + \frac{4\pi^{1/2}(Nr)}{3} \sum_{n=0}^{\infty} \frac{A_{2n}}{(n+2)} \exp[-(n+1)z^*], \tag{3.11}$$

$$T_1(z^*) = T_{10} + \sum_{n=0}^{\infty} \left[\frac{16\pi(Nr)^2 A_{2n}}{(n+2)^2} \exp[-(n+2)z^*] - 2A_{2n} \exp(-nz^*)\right], \tag{3.12}$$

$$\rho_1(z^*) = \rho_{10} + T_{10}z^* - 4\pi\epsilon_G(Nr)\exp(-z^*) + \sum_{n=1}^{\infty} \left[\frac{-(n+1)}{n}(T_{1n} + 2A_{2n})\exp(-nz^*)\right]. \tag{3.13}$$

The constant A_{20} is determined using the boundary condition (2.64), while the constants T_{10} and ρ_{10} are determined using the integral condition for the density (2.59) and the integral condition for the energy balance (2.60) with the source and dissipation of energy given by (2.61) and (2.63) respectively. The $O(\epsilon_D)$ correction to the moments of the distribution function are determined by substituting the above solutions for the functions $A_1(z^*), A_2(z^*), A_3(z^*), T_1(z^*)$ and $\rho_1(z^*)$ into the equations (2.22)–(2.26).

The anisotropy in the distribution function $\langle u_z^{*2} - u_x^{*2}\rangle$ is shown as a function of z^* for different values of Nr in figure 2(*a*), and the third moments of the distribution function $\langle u_z^{*3}\rangle$ and $\langle u_x^{*2}u_z^*\rangle$ are shown in figure 2(*b, c*). The $z^* \to \infty$ behaviour of the third moments of the velocity distribution in the present case are very different from those for a suspension where the dissipation is due to inelastic collisions. The balance between the conduction of energy due to the third moment of the distribution function in (2.28) and (2.29), proportional to $\rho_0^*\langle u_z^{*3}\rangle$ and $\rho_0^*\langle u_x^{*2}u_z^*\rangle$, and the viscous dissipation of energy, proportional to ρ_0^*, requires that the third moments attain constant values independent of Nr in the limit $z^* \to \infty$. In addition, the rates of dissipation of energy in the horizontal and vertical directions are equal, therefore the limiting values of the third moments of the velocity distribution are also equal.

The collisional transport of energy from the vertical to the horizontal direction, which is proportional to $\rho_0^{*2}\langle u_z^{*2} - u_x^{*2}\rangle$, is small compared to the conduction of energy in the limit $z^* \to \infty$. In addition, the limiting value of the anisotropy in the distribution function, $\langle u_z^{*2} - u_x^{*2}\rangle$, is independent of Nr in the present case. This is because the leading-order rate of transport of energy due to collisions, which is proportional to

ρ_0^{*2}, is balanced by the $O(\exp(-z^*))$ correction to the rate of conduction of energy in (2.39) and (2.40), which is also proportional to Nr.

The first corrections to the temperature and density are expressed as $T_1 = T_1' + (\epsilon_G/\epsilon_D)T_1''$ and $\rho_0\rho_1 = \rho_1'(z^*) + (\epsilon_G/\epsilon_D)\rho_1''(z^*)$. In the present case, the function $T_1'' = -4.1888Nr$ is independent of z^*, and the functions T_1', ρ_1' and ρ_1'' are shown as functions of z^* in figure 2(*d–f*). The trend exhibited by these functions is very similar to that for a suspension where the dissipation is due to inelastic collisions. The functions T_1'' and ρ_1'' are larger than T_1' and ρ_1' in the present case also, indicating that the effect of variation in the gradients in the concentration field on collisional interactions dominates the effect of the perturbation to the distribution function for $\epsilon_G/\epsilon_D \sim 1$.

3.3. *Comparison with experimental results*

There have been a relatively small number of experimental studies and numerical simulations that have attempted to examine the particle distribution functions in the uniform state of a vibrated fluidized bed. Luding *et al.* (1994) carried out event-driven simulations of a vibrated fluidized bed of inelastic particles, and reported the behaviour of the density variation in the bed. However, they did not provide the magnitudes of the velocity fluctuations, so it is difficult to make a rigorous comparison with their results. Details of the velocity distribution were determined experimentally using imaging techniques by Warr *et al.* (1995) for a two-dimensional bed of particles, and their experimental results are compared with the predictions of the analysis in the present section.

The experimental system of Warr *et al.* (1995) consisted of a two-dimensional bed of spherical particles of diameter 5 mm confined between two glass plates separated by a distance of 5.05 mm. The bed was vibrated at the bottom with a frequency of 50 Hz and an amplitude between 0.5 and 2.12 mm. The coefficient of restitution for binary collisions between the particles was reported as 0.92, and the parameter values Nr for the different experiments are given in table 1. It can also be seen from table 1 that the parameter $\epsilon = U_0^2/T_0$ is not small in the experiments, and could be greater than 1.0 in some cases. Thus, quantitative agreement between the experiments and analysis cannot be expected, and in the present section a qualitative comparison is made between the experimental and analytical results.

The experimental results for the scaling of the temperature with the maximum velocity of the vibrating base is $T \propto U_0^{\alpha}$, where α is reported to be between 1.36 and 1.41. This is in between the analytical predictions of the previous section of $\alpha = 1.33$ for a system where viscous drag is the dominant mechanism, and $\alpha = 2.0$ for a system where inelastic collisions are the dominant mechanism of dissipation of energy. Thus, it appears that both inelastic collisions and viscous drag are important, and the temperatures observed in the experiments are in good agreement with those of the analysis for $\mu/g = 0.35$ m^{-1} s, as shown in table 1. The agreement is poor for the lowest number density used in the experiments, but it should be noted that at this number density, the number of particles is sufficient for less than one monolayer on the surface at rest. The analysis may not be applicable in this case because the probability of particle collisions with the vibrating surface is more than the probability of binary collisions, and the assumption of molecular chaos used in the analysis may not be valid. In the remainder of this subsection, the analytical results are derived assuming that the dissipation of energy is due to both inelastic collisions and viscous drag, and using $\mu/g = 0.35$ m^{-1} s.

The comparison of the area fraction profiles is shown in figure 3 for the experimental parameters listed in table 1. It is observed that the qualitative features of the analytical

Experiment Number	Nr	U_0 (m s^{-1})	T_e (m^2 s^{-2})	$\epsilon_e = U_0^2/T_e$	T_a (m^2 s^{-2})	$\epsilon_G = rg/T_e$
1	0.4091	0.1571	0.0849	0.2907	0.0672	0.2888
2	0.4091	0.3519	0.2837	0.4365	0.2234	0.0865
3	0.4091	0.5781	0.5505	0.6071	0.4563	0.0446
4	0.4091	0.6660	0.8413	0.5272	0.5580	0.0292
5	0.6061	0.1571	0.0612	0.4033	0.0588	0.4007
6	0.6061	0.3519	0.2026	0.6112	0.2050	0.1211
7	0.6061	0.5781	0.4255	0.7854	0.4280	0.0576
8	0.6061	0.6660	0.5374	0.8254	0.5261	0.0456
9	0.9091	0.1571	0.0488	0.5058	0.0489	0.5026
10	0.9091	0.3519	0.1759	0.7843	0.1812	0.1394
11	0.9091	0.5781	0.3594	0.9299	0.3896	0.0682
12	0.9091	0.6660	0.4660	0.9518	0.4824	0.0526
13	1.3636	0.1571	0.0394	0.6264	0.0387	0.6225
14	1.3636	0.3519	0.1346	0.9200	0.1531	0.1822
15	1.3636	0.5781	0.3342	1.0000	0.3416	0.0734
16	1.3636	0.6660	0.3927	1.1295	0.4271	0.0625

TABLE 1. The parameters Nr, U_0, the observed temperature T_e and the parameter U_0^2/T_e used in the experiments of Warr *et al.* (1995), and the temperature T_a predicted by the analysis for $\mu/g = 0.35$.

predictions are in good qualitative agreement with the experimental results for all the parameter values, except for the experiments at the lowest density where, as indicated earlier, the approximation of molecular chaos may not be valid. It is experimentally observed that the area fraction initially increases and then shows an exponential decrease as the height is increased, in agreement with the results of the analysis. In addition, the analytical predictions are in good quantitative agreement with the experimental results for values of U_0^2/T_0 less than 0.5, using just one adjustable parameter (μ/g) which has been fitted to obtain the correct temperature. The analytical predictions for the anisotropy in the distribution function are compared with experimental results in figure 4. As seen from figure 4, the experimental results show a lot of scatter, and the error bars are quite large, sometimes equal to half the value of the temperature itself. Therefore, it is difficult to make a rigorous comparison of the analytical and experimental results for the anisotropy. However, from figure 4, it can be inferred that the experimental results for the anisotropy are of the same magnitude as the theoretical predictions, and the vertical temperature is greater than that in the horizontal direction in both the analysis and the experiments. Warr *et al.* (1995) do not report any results for the skewness of the distribution function, but it is apparent from their distribution functions (figures 3 and 4 of their paper) that the skewness in the distribution of velocities in the vertical direction is positive, and the magnitude of the skewness decreases and the distribution function becomes symmetric as the height is increased. These observations are in qualitative agreement with the results of the predictions of the analysis for the density profile, anisotropy and the third moments of the distribution, though quantitative agreement is not observed because the parameters ϵ_I and ϵ_D are not small in the experiments.

4. Conclusions

The distribution function for a vibro-fluidized bed was calculated using asymptotic analysis in the limit where the dissipation of energy in a collision due to inelasticity

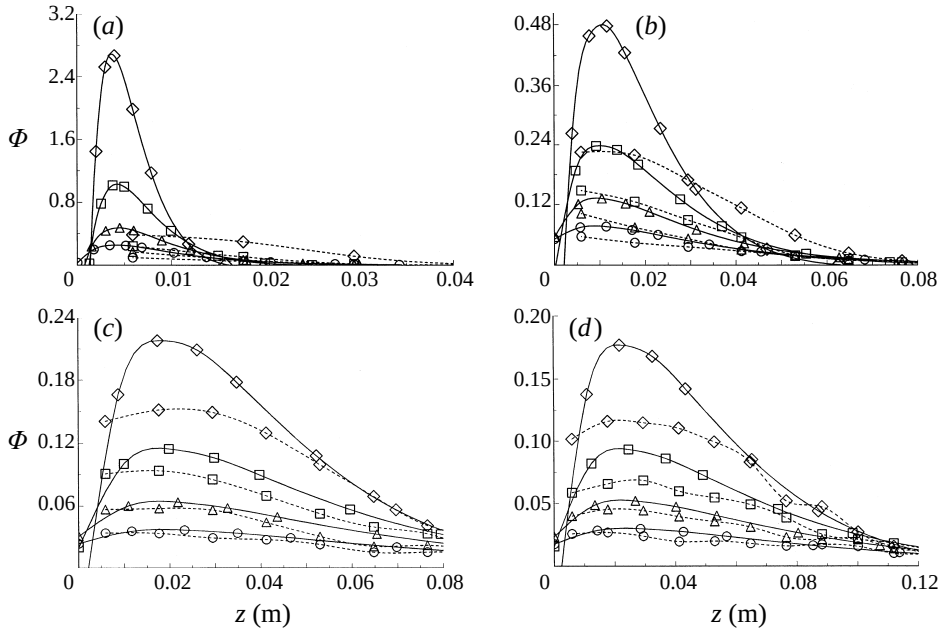

FIGURE 3. Comparison between the density profiles predicted by the present analysis and those reported by Warr *et al.* (1995). The solid lines represent the analytical results, and the broken lines represent the experimental results. The data points correspond to the parameter values for the following experiments listed in table 1: (*a*) ○, 1; △, 5; □, 9; ◇, 13. (*b*) ○, 2; △, 6; □, 10; ◇, 14. (*c*) ○, 3; △, 7; □, 11; ◇, 15. (*d*) ○, 4; △, 8; □, 12; ◇, 16.

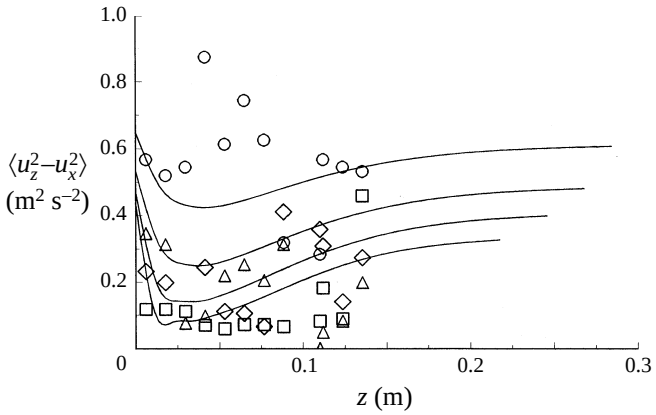

FIGURE 4. Comparison between the anisotropy in the mean-square velocity predicted by the present analysis and that reported by Warr *et al.* (1995). The solid lines represent the analytical results, and the scattered data points represent the experimental results. The data points correspond to the following experiments listed in table 1: ○, 4; △, 8; □, 12; ◇, 16.

or between successive collisions due to viscous drag is small compared to the energy of a particle. In addition, the radius of a particle is considered to be small compared to the length scale of variation of density. In the leading approximation, the system is identical to a gas of point particles in a gravitational field which undergo elastic collisions. The density is given by the Boltzmann distribution, and the velocity distribution function is given by the Maxwell–Boltzmann distribution with a constant

temperature. However, the temperature is not specified in the leading approximation, and has to be determined by a balance between the source of energy at the vibrating surface and the dissipation due to viscous drag or inelastic collisions. The correction to the distribution function due to dissipation and density variation is considered to be in the form of the product of the leading-order distribution and an expansion in the moments of the velocity components, and all non-trivial first, second and third moments are included in the expansion. The parameters in the expansion, as well as the correction to the temperature and density, are determined analytically.

Richman & Martin (1992) provided a continuum description of a vibro-fluidized bed, where they used a momentum conservation equation in the vertical direction and an energy conservation equation for describing the dynamics of the bed. The constitutive relations for the energy transport were adapted from a constitutive theory of Jenkins & Richman (1985). Continuum theories based on the Chapmen–Enskog theory for dense gases have also been used earlier for shear flows of suspensions. It is useful to examine the advantages of the present analysis in comparison to the earlier continuum theories. In the continuum theory of Richman & Martin (1992), the mass conservation equation states that the velocity in the vertical direction is identically zero. The momentum conservation equation is a first-order differential equation relating the gradient in the pressure in the vertical direction to the density at steady state

$$\frac{\partial p}{\partial z} = \rho g$$

where the pressure is related to the temperature by an equation of state. The energy conservation equation relates the energy flux to the rate of dissipation of energy

$$\frac{\partial}{\partial z} K \frac{\partial T}{\partial z} - D(z) = 0$$

where $D(z)\mathrm{d}z$ is the dissipation of energy due to inelastic collisions or viscous drag in the interval $\mathrm{d}z$ about z. The solution of the above two equations requires a total of three boundary conditions. However, there are at least four conditions required to be satisfied by the physical system:

(*a*) the density $\rho \to 0$ as $z \to \infty$;

(*b*) the energy flux $(\partial T/\partial z) \to 0$ as $z \to \infty$;

(*c*) the energy flux $(\partial T/\partial z)$ has a value specified by the conditions at the vibrating surface at $z = 0$;

(*d*) the total mass of the material per unit length of the bed is fixed by the amount of material originally put in.

All of these cannot be simultaneously enforced by the continuum model, and one needs a more detailed model for a realistic description of the vibro-fluidized bed. Richman & Martin resolved this problem by specifying a 'height' β for the bed, which was a free parameter. The addition of this free parameter enabled them to satisfy the fourth boundary condition as well. However, there is no such height in the present system, and the density decreases exponentially with height. Consequently, one cannot satisfy all the boundary conditions which one would expect the physical system to satisfy.

A more detailed continuum description would involve separate conservation equations for the temperatures (mean-square velocities) in the vertical (T_z) and horizontal (T_x) directions. With this type of description, there are two difficulties. One is that the Chapman–Enskog dense gas theory does not specify the correct form for the thermal conductivity separately in the horizontal and vertical directions. The second

is that the number of boundary conditions required for obtaining a solution is still smaller than those that one would reasonably expect the physical system to satisfy. This description gives two second-order differential equation for the velocities in the horizontal and vertical direction, and a first-order differential equation for the momentum. These equations require five boundary conditions to specify a unique solution. However, there are at least six boundary conditions that one would reasonable expect the physical system to satisfy:

(*a*) the density $\rho \to 0$ as $z \to \infty$;

(*b*) the vertical temperature $T_z \to 0$ as $z \to \infty$;

(*c*) the horizontal temperature $T_x \to 0$ as $z \to \infty$;

(*d*) a relation for the flux of the vertical temperature $(\partial T_z/\partial z)$ at the vibrating surface;

(*e*) a relation for the flux of the horizontal temperature $(\partial T_x/\partial z)$ at the vibrating surface;

(*f*) the total mass condition.

Consequently, a more detailed description of the type provided here is required for enforcing all the boundary conditions that one would reasonable require the physical system to satisfy.

The analysis indicates that there are some systematic deviations due to dissipation which are independent of the dissipation mechanism. The magnitude of the correction to the density is largest at the vibrating surface, and the density correction is negative near the bottom of the bed. The correction to the density increases and assumes positive values as the height is increased, and decreases to zero exponentially at large heights. The correction to the temperature is positive at the bottom, and decreases and becomes negative near the top. In addition, the mean-square velocity in the vertical direction is larger than that in the horizontal direction. These qualitative features have been observed in the experiments of Warr *et al.* (1995), and the decrease in density near the bottom has also been reported in the simulations of Luding *et al.* (1994). There are also some significant differences in the variation of the velocity moments for systems with dissipation due to inelastic collisions and viscous drag. The anisotropy in the second moments, as well as the non-zero third moments of the distribution function, decrease exponentially with height for a system where dissipation is due to inelastic collisions, but they assume a constant value at large heights for a system where dissipation is due to viscous drag. These qualitative differences do not seem to have been probed in experiments or simulations.

The author would like to thank Dr S. Warr for introducing him to this problem and for instructive discussions, and Dr S. Luding for useful discussions.

REFERENCES

Batchelor, G. K. 1988 A new theory of the instability of a fluidized bed. *J. Fluid Mech.* **193**, 75–110.

Cercignani, C. 1975 *The Boltzmann Equation and Its Applications.* Springer.

Didwania, A. K. & Homsy, G. M. 1982 Resonant sideband instabilities in wave propagation in fluidized beds. *J. Fluid Mech.* **122**, 433–438.

Goldshtein, A., Shapiro, M., Moldavsky, L. & Fichman M. 1995 Mechanics of collisional motion of granular materials. Part 2. Wave propagation through vibro-fluidized granular layers. *J. Fluid Mech.* **287**, 349–382.

Hoover, W. G. & Alder, B. J. 1967 Studies in molecular dynamics. IV. The pressure, collision rate, and their number dependence for hard disks. *J. Chem. Phys.* **46**, 686–691.

Jackson, R. 1963 The mechanics of fluidized beds. Parts 1 and 2. *Trans. Inst. Chem. Engrs* **41**, 13–28.

Jackson, R. 1985 Hydrodynamic stability of fluid-particle systems. In *Fluidization* (ed. J. F. Davidson, R. Clift & D. Harrison). Academic.

Jenkins, J. T. & Richman, M. W. 1985 Grad's 13 moment system for a dense gas of inelastic spheres. *Arch. Rat. Mech. Anal.* **87**, 355–377.

Jenkins, J. T. & Richman, M. W. 1986, Boundary conditions for plane flows of smooth, nearly elastic circular disks. *J. Fluid Mech.* **171**, 53–69.

Jenkins, J. T. & Savage, S. B. 1983 A theory for the rapid flow of identical, smooth, nearly elastic, spherical particles. *J. Fluid Mech.* **130**, 187–202.

Johnson, P. C. & Jackson, R. 1987 Frictional–collisional constitutive relations for granular materials, with application to plane shearing. *J. Fluid Mech.*, **176**, 67–93.

Kumaran, V. 1998 Temperature of a granular material fluidized by external vibrations. *Phys. Rev.* E (in Press).

Luding, S., Herrmann, H. J. & Blumen, A. 1994 Simulations of two-dimensional arrays of beads under external vibrations: Scaling behaviour. *Phys. Rev.* E **50**, 3100–3108.

Lun, C. K. K., Savage, S. B., Jeffrey, D. J. & Chepurniy, N. 1984 Kinetic theories for granular flow: inelastic particles in Couette flow and slightly inelastic particles in a general flow field. *J. Fluid Mech.* **140**, 223–256.

Richman, M. W. & Martin, R. E. 1992 The effects of anisotropic boundary vibrations on confined, thermalized, granular assemblies. *Proc. of the Ninth ASCE Engineering Conference* (ed. L. T. Lutes & J. M. Niedzwedki), pp. 900–903.

Savage, S. B. 1988 Streaming motions in a bed of vibrationally fluidized dry granular material, *J. Fluid Mech.* **194**, 457–478.

Sirovich, L. & Thurber, J. K. 1965, Propagation of forced sound waves in rarefied gasdynamics. *J. Acoust. Soc. Am.* **37**, 329–339.

Verlet, S. & Levesque, D. 1982 Integral equations for classical fluids III. The hard discs system. *Mol. Phys.* **46**, 969–980.

Warr, S., Huntley, J. M. & Jacques, G. T. H. 1995 Fluidization of a two dimensional granular system: Experimental study and scaling behaviour. *Phys. Rev.* E **52**, 5583–5595.